NANO LETTERS

Letter

pubs.acs.org/NanoLett

Observation of Rapid Exciton−Exciton Annihilation in Monolayer Molybdenum Disulfide

Dezheng Sun,[†,#] Yi Rao,[†,‡,#] Georg A. Reider,[§] Gugang Chen,[∥] Yumeng You,[†] Louis Brézin,[⊥] Avetik R. Harutyunyan,[∥] and Tony F. Heinz*[,†]

[†]Departments of Physics and Electrical Engineering, Columbia University, New York, New York 10027, United States

[‡]Department of Chemistry, Temple University, Philadelphia, Pennsylvania 19122, United States

[§]Photonics Institute, TU Wien, Gusshausstrasse 27-387, A 1040 Wien, Austria

[∥]Honda Research Institute USA, Inc., Columbus, Ohio 43212, United States

[⊥]Laboratoire d'Optique Appliquée, ENSTA, CNRS, Ecole Polytechnique, 91761 Palaiseau, France

Supporting Information

ABSTRACT: Monolayer MoS_2 is a direct-gap two-dimensional semiconductor that exhibits strong electron−hole interactions, leading to the formation of stable excitons and trions. Here we report the existence of efficient exciton−exciton annihilation, a four-body interaction, in this material. Exciton−exciton annihilation was identified experimentally in ultrafast transient absorption measurements through the emergence of a decay channel varying quadratically with exciton density. The rate of exciton−exciton annihilation was determined to be $(4.3 \pm 1.1) \times 10^{-2}$ cm^2/s at room temperature.

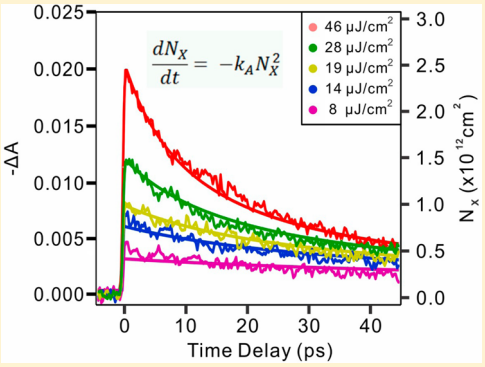

KEYWORDS: *MoS_2, transient absorption spectroscopy, exciton dynamics, exciton−exciton annihilation*

Monolayers of transition metal dichalcogenides (TMDs), including MoS_2, $MoSe_2$, WS_2, and WSe_2, have recently attracted much interest as a new class of atomically thin materials.[1−4] Like graphene, these materials are environmentally stable and can be prepared both by exfoliation of bulk crystals and by chemical synthesis. In contrast to graphene, however, these two-dimensional (2D) materials exhibit a significant band gap. In addition, in the single-layer limit the crystals are direct-gap semiconductors and support efficient light emission.[5,6] These materials are also of particular interest because they display distinctive valley-selective optical properties.[4,7−11] A consequence of the quantum confinement and reduced dielectric screening in atomically thin 2D materials is the role of strong Coulomb interactions between carriers.[12−16] This leads to tightly bound excitons upon photoexcitation of the material. Indeed, the strength of the Coulomb interaction in these materials is sufficient to support charged excitons (trions), even at room temperature, in doped material.[17,18]

In this paper, we identify and characterize the exciton−exciton annihilation process in single-layer MoS_2. Exciton−exciton annihilation is a many-body interaction in which one exciton (or electron−hole pair) is destroyed and its energy transferred to another exciton. This annihilation channel for photoexcited material is the excitonic analog of the Auger recombination process, a well-known nonradiative decay mechanism operative in highly excited semiconductors with free charge carriers. Exciton−exciton annihilation and Auger recombination are particularly significant in systems of reduced dimensionality, as observed in quantum wells,[19−21] quantum dots,[22] and carbon nanotubes.[23−26] Exciton−exciton annihilation is expected to be efficient in an atomically thin 2D material like single-layer MoS_2 with strong many-body interactions.[27]

Our study of exciton−exciton annihilation in single-layer MoS_2 was performed by means of ultrafast transient absorption spectroscopy. We find dynamics of the band-edge (A) exciton over a broad range of densities can be successfully modeled by a decay channel that varies quadratically with exciton density. We infer an exciton−exciton annihilation rate of $(4.3 \pm 1.1) \times 10^{-2}$ cm^2/s for single-layer MoS_2 at room temperature. This rate of exciton−exciton annihilation is higher than in conventional layered materials. Beyond the fundamental interest in this many-body process, exciton−exciton annihilation is important because it defines the maximum excitation density that can be achieved in the material under different pumping schemes. Such nonradiative recombination channels frequently influence the efficiency of semiconductor lasers and light-emitting diodes.

Received: June 12, 2014
Revised: August 23, 2014
Published: August 29, 2014

   dx.doi.org/10.1021/nl5021975 | *Nano Lett.* 2014, 14, 5625−5629

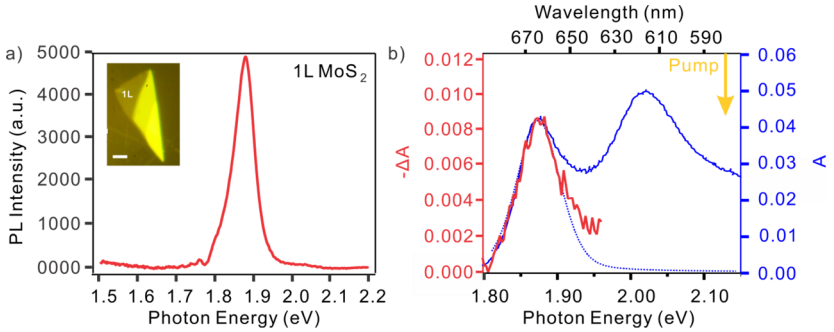

Figure 1. (a) Photoluminescence spectrum of monolayer MoS_2 at room temperature under cw laser excitation at a wavelength of 532 nm. The sideband of photoluminescence located at lower energy side is due to the trion emission. Hot photoluminescence from the higher-lying B exciton transition can be seen at around 2.0 eV. The optical image in the inset shows a monolayer sample exfoliated on quartz substrate. The scale bar is 5 μm. (b) Transient reflectivity spectrum measured at a time delay of 0.2 ps for monolayer sample. For comparison, the absorption spectrum is shown for the unpumped sample. The dotted line represents the contribution to the absorption spectrum from the A exciton based on a fit to two Lorentzian peaks for the A and B excitons and a linear background.

Exciton−exciton annihilation is also important as the time-reversed image of the process of multiple-exciton generation. The high efficiency of the exciton−exciton annihilation process reported here suggests that TMD materials may be particularly well suited for multiple-exciton generation and, correspondingly, as candidate materials for advanced photovoltaic devices.

Monolayer MoS_2 crystals were prepared on fused quartz substrates by means of mechanical exfoliation from bulk crystal of molybdenite (SPI). The single-layer samples were identified by optical microscopy (inset, Figure 1a) and their thickness was confirmed by Raman and photoluminescence spectroscopy.[5,6,28] Figure 1a presents the photoluminescence spectrum of a typical monolayer MoS_2 sample at room temperature. The dominant emission feature at 1.88 eV is the band-edge (A) exciton[5,6] Because of the unintentional doping, a small emission feature also appears at low-energy side of the peak, which corresponds to the negatively charged exciton. Very weak hot luminescence from the B exciton can be seen at a photon energy around 2.05 eV.

Transient optical spectra for MoS_2 monolayers were obtained using pump pulses at 2.14 eV. The response was probed with ultrafast supercontinuum pulses, covering photon energies from 2.07 to 1.65 eV. The pump and probe pulses were generated by an amplified modelocked fiber laser (Impulse, Clarke-MXR) operating at a wavelength of 1.03 μm and a repetition rate of 1 MHz. The broad supercontinuum light was produced by focusing laser pulses of ~1 μJ energy in an undoped YAG crystal. The pump radiation was obtained by passing the supercontinuum radiation through a band-pass filter centered at 2.14 eV with a bandwidth of 0.04 eV. A less intense unfiltered supercontinuum radiation served as a broadband probe. For the time-resolved data presented in this paper, we chose to measure the response at the peak of the A exciton, that is, at a photon energy around 1.88 eV. The cross-correlation width for the pump and probe pulses was 300 fs.

The transient spectroscopy measurements were performed with collinear pump and probe beams. The beams were focused on the MoS_2 sample with a 50× long-working distance objective, producing a spot diameter of 2 μm. (The method for determining the effective pump fluence in our measurements is described in the Supporting Information.) The reflected probe beam was collected by the same objective, passed through a monochromator, and detected by a Si photodiode. The pump beam was chopped at 700 Hz and the resultant modulation of the probe beam was measured by lock-in techniques. A differential change of 10^{-3} in reflected probe intensity could be measured with a 3 s integration time.

In our experiments, we measure the reflectivity R or the change in reflectivity ΔR from the sample. Because the influence of the MoS_2 layer on the reflection from the fused quartz substrate is relatively weak, we can make use of a simple relation to determine the absorption A of the MoS_2 monolayer from fractional change in the reflectivity[29]

$$\frac{\Delta R}{R} = \frac{4A}{n_s^2 - 1} \quad (1)$$

Here n_s = 1.50 denotes the refractive index of the transparent substrate. We use this relation to obtain the absolute absorption spectrum of the MoS_2. For the pump−probe measurements, we apply the same relation to determine the pump-induced change ΔA in the absorption of the MoS_2 layer.

We first consider the spectral response induced in monolayer MoS_2 by a femtosecond excitation pulse. Figure 1b displays the absorption spectrum A of the unexcited MoS_2 layer and the photoinduced change in the absorption ΔA. The absorption spectrum shows two prominent features, corresponding to the A exciton, centered at 1.88 eV, and the higher-lying B exciton, centered at 2.05 eV. The dotted line represents the contribution of the A exciton to the overall absorption spectrum, based on a simple decomposition into Lorentzian line shapes. The photoinduced change in the absorption, measured at a time delay of 200 fs, is seen to closely follow the profile of the A exciton absorption. Within experimental accuracy, there is no significant shift in the position of the A exciton or change in width under photoexcitation at these levels. Rather, we simply see a reduction in the strength of the feature ($\Delta A < 0$). We have performed analogous measurements of the transient spectra (not shown) at subsequent delay times and observed similar behavior, indicating that the interpretation, discussed below, is appropriate for all delay times.

We attribute the observed reduction in absorption to the presence of A excitons. For the range of applied pump fluences (8−46 μJ/cm^2) in our experiment, we find that the induced change in the signal scales linearly with fluence (Supporting Information Figure S4). We infer from this observation that the absorption of the pump radiation remains independent of fluence, as expected for rapid relaxation of the B exciton, and

dx.doi.org/10.1021/nl5021975 | Nano Lett. 2014, 14, 5625−5629

also that the bleaching of the sample remains linear in the exciton density over our experimental range of conditions.

We present transient reflection/absorption data obtained for a probe photon energy of 1.88 eV, corresponding to measurements at the peak of the A exciton absorption. On the basis of the discussion above, we interpret the change in absorption as proportional to the density of A excitons in the MoS_2 monolayer. To gauge the pump-induced perturbation of the material, let us consider the conditions of Figure 1b with an applied pump fluence of 22 $\mu J/cm^2$. Taking into account the change in the applied field arising from the reflection from the substrate and the absorption of the MoS_2 monolayer at the pump wavelength (2.7%), this excitation corresponds to an absorbed fluence of 0.39 $\mu J/cm^2$. Assuming that each absorbed photon generates one A exciton, the resulting initial exciton density is 1.1×10^{12} cm^{-2}, that is, an average separation between excitons of 9.5 nm.

Figure 2a shows the transient absorption of monolayer MoS_2 for applied pump fluences of 22 and 3 $\mu J/cm^2$. The probe photon energy is chosen as resonant with A-exciton absorption. The transient absorption at the higher fluence shows a multiexponential decay. It can be adequately fit using a sum of two exponential terms with decay times of 19 and 105 ps. Similar nonexponential decays have been reported in pump–probe[30−35] and time-resolved fluorescence[36,37] studies of MoS_2 and other monolayer TMD materials. Various assignments have been made to the different decay times, including trapping at defect sites and carrier cooling processes. For the tightly bound A excitons, we would not expect these processes to exhibit a rate that depends strongly on exciton density, although saturation effects might lead the trap-related decay to become more prominent at lower exciton density. In fact, in the studies in the literature no strong or systematic variation with fluence was identified under the chosen experimental conditions. In our case, however, we see that at a reduced pump fluence of 3 $\mu J/cm^2$ the decay rate becomes considerably slower. Within the experimental accuracy, the data can be fit to a single exponential decay with a 360 ps time constant.

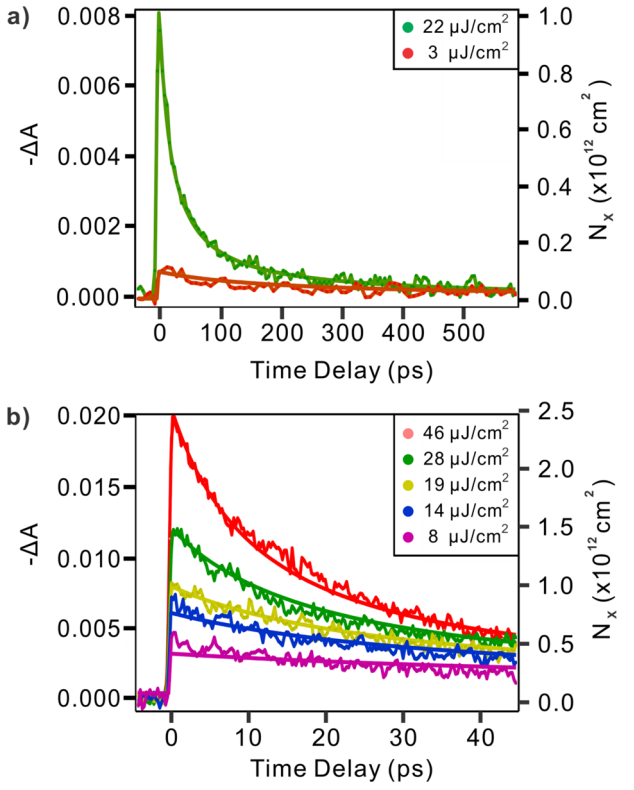

Figure 2. (a) Transient reflectivity of monolayer MoS_2 at room temperature measured at two pump fluences of 22 and 3 $\mu J/cm^2$ with a time scale of 600 ps. (b) Exciton dynamics at different pump fluences with a time scale of 45 ps. The right axis corresponds to photogenerated excitons. The solid lines represent a global fit to the exciton–exciton annihilation model as seen in eq 3, by convoluting with experimental instrumental response function.

To explore the strong dependence of the decay dynamics on the initial exciton density in detail, we have performed time-resolved measurements of the absorption for a range of pump fluences. The results are shown in Figure 2b. To fit these data to exponential decays would not only require at least two exponential terms but also a changing of ratio between different components with fluence. (Please see the Supporting Information Section S1 Figures S1–S3, Tables S1 and S2 for a detailed analysis of single and biexponential fits of the experimental data.)

Instead, we show here that the entire set of data for the exciton dynamics can be fit by a simple model based on exciton–exciton annihilation. We model the process by decay kinetics in which we include a loss term for exciton population $N_X(t)$ that varies quadratically in the exciton density, as expected for the exciton–exciton annihilation process

$$\frac{dN_X}{dt} = -k_A N_X^2 \tag{2}$$

with k_A representing the rate constant for the annihilation process. The solution to eq 2 is

$$N_X(t) = \frac{N_0}{1 + k_A N_0 t} \tag{3}$$

where N_0 is the initial photogenerated exciton population.

This simple model of the decay dynamics provides a good fit to the complete set of experimental data, as indicated by the solid lines in Figure 2a,b. Considering all sets of data, we obtain an annihilation rate of $k_A = (4.3 \pm 1.1) \times 10^{-2}$ cm^2/s. This result implies an effective lifetime for excitons in monolayer MoS_2 of 11 ps at an exciton density of 1×10^{12} cm^{-2} or an average carrier separation of 10 nm. The model that we have introduced for exciton dynamics provides a good global fit to the entire set of transient absorption data for different initial exciton densities. It is based solely on decay by exciton–exciton annihilation. Of course, there are additional density-independent channels for exciton decay, including radiative recombination and defect-mediated relaxation channels. These will dominate for sufficiently low exciton density. Indeed, inspection of the transient absorption decay curve in Figure 2 at the lowest pump fluence reveals that the predicted decay based solely on exciton–exciton annihilation underestimates the observed decay rate. We can improve the fit of the data for low exciton concentrations by adding to the exciton–exciton annihilation term in rate eq 2 a density-independent decay with a time constant of 90 ps. We attribute this decay channel to nonradiative processes associated with traps and impurities. With respect to the role of radiative decay, samples prepared in the same way as our MoS_2 monolayers have a room-temperature quantum yield of less than 1%.[1,6] On the basis of our measured low-fluence exciton decay time constant of

dx.doi.org/10.1021/nl5021975 | Nano Lett. 2014, 14, 5625–5629

~100 ps, we infer that the exciton radiative decay will have a lifetime exceeding 10 ns. Radiative decay, while obviously present, is therefore not significant in the analysis of the current transient absorption data.

Another process that is expected to display a rate that is quadratic in the exciton density is biexciton formation. Although we have recently observed signatures of biexcitons in transition metal dichalcogenides at cryogenic temperatures, there is no evidence of significant biexciton population at room temperature.[38]

It is illuminating to compare the exciton−exciton annihilation process in monolayer MoS_2 to that observed for carriers in conventional semiconductor III−V quantum well systems. At room temperature, photoexcitation in III−V quantum wells leads to free carriers, rather than to excitons; the corresponding annihilation process is normally described as a three-body Auger recombination process. We can nonetheless compare the influence of many-body interactions in creating nonradiative pathways by considering the decay rate for an average carrier separation of 10 nm. In contrast to the measured lifetime of 11 ps for MoS_2, we expect a lifetime of 1.1 μs, where we consider a typical III−V material with a band gap comparable to the A exciton energy in MoS_2 with Auger coefficient of 1×10^{-31} cm^6 s^{-1}.[39] While such comparisons have a certain arbitrariness, given the different scaling of rates with carrier density, we see that many-body effects play a much more dramatic role in nonradiative decay processes in the atomically thin MoS_2 monolayer than in conventional semiconductor systems. We attribute this difference to the strong confinement effects in the monolayer limit and the associated reduced dielectric screening.

We have measured transient optical absorption of monolayer MoS_2 at room temperature under conditions of different pump fluence. Fluence-dependent dynamics showed a pronounced exciton−exciton annihilation process over the whole carrier decay signal. A bimolecular recombination model was used to account for the exciton−exciton annihilation process. The rate for the annihilation was found to be as large as $(4.3 \pm 1.1) \times 10^{-2}$ cm^2/s. These results help us to understand many-body interactions in a two-dimensional material. In addition, this fast exciton−exciton annihilation acts to limit the carrier density a monolayer MoS_2 can sustain under different excitation conditions, an important factor for designing optoelectronic devices based on transition metal dichalcogenide layers.

■ ASSOCIATED CONTENT

Supporting Information

Figures S1−S4, and Tables S1−S2 as described in the text. This material is available free of charge via the Internet at http://pubs.acs.org.

■ AUTHOR INFORMATION

Corresponding Author

*E-mail: tony.heinz@columbia.edu.

Author Contributions

#D.S. and Y.R. contributed equally to this work.

Notes

The authors declare no competing financial interest.

■ ACKNOWLEDGMENTS

The authors at Columbia University acknowledge support from the National Science Foundation (Grants DMR-1122594 and DMR-1106172) for the spectroscopy measurements, from the Columbia Energy Frontier Research Center funded by the U.S. Department of Energy (DOE), Office of Science, Office of Basic Energy Sciences under Award DE-SC0001085 and the Keck Foundation for sample preparation and characterization, and from the Honda Research Institute, USA.

■ REFERENCES

(1) Wang, Q. H.; Kalantar-Zadeh, K.; Kis, A.; Coleman, J. N.; Strano, M. S. *Nat. Nanotechnol.* **2012**, *7*, 699.
(2) Chhowalla, M.; Shin, H. S.; Eda, G.; Li, L.-J.; Loh, K. P.; Zhang, H. *Nat. Chem.* **2013**, *5*, 263.
(3) Butler, S. Z.; et al. *ACS Nano* **2013**, *7*, 2898.
(4) Xu, X.; Yao, W.; Xiao, D.; Heinz, T. F. *Nat. Phys.* **2014**, *10*, 343.
(5) Splendiani, A.; Sun, L.; Zhang, Y.; Li, T.; Kim, J.; Chim, C.-Y.; Galli, G.; Wang, F. *Nano Lett.* **2010**, *10*, 1271.
(6) Mak, K. F.; Lee, C.; Hone, J.; Shan, J.; Heinz, T. F. *Phys. Rev. Lett.* **2010**, *105*, 136805.
(7) Xiao, D.; Liu, G.-B.; Feng, W.; Xu, X.; Yao, W. *Phys. Rev. Lett.* **2012**, *108*, 196802.
(8) Cao, T.; et al. *Nat. Commun.* **2012**, *3*, 887.
(9) Mak, K. F.; He, K.; Shan, J.; Heinz, T. F. *Nat. Nanotechnol.* **2012**, *7*, 494.
(10) Zeng, H.; Dai, J.; Yao, W.; Xiao, D.; Cui, X. *Nat. Nanotechnol.* **2012**, *7*, 490.
(11) Jones, A. M.; et al. *Nat. Nanotechnol.* **2013**, *8*, 634.
(12) Berkelbach, T. C.; Hybertsen, M. S.; Reichman, D. R. *Phys. Rev. B* **2013**, *88*, 045318.
(13) Qiu, D. Y.; da Jornada, F. H.; Louie, S. G. *Phys. Rev. Lett.* **2013**, *111*, 216805.
(14) Cheiwchanchamnangij, T.; Lambrecht, W. R. L. *Phys. Rev. B* **2012**, *85*, 205302.
(15) Ramasubramaniam, A. *Phys. Rev. B* **2012**, *86*, 115409.
(16) Komsa, H.-P.; Krasheninnikov, A. V. *Phys. Rev. B* **2012**, *86*, 241201.
(17) Mak, K. F.; He, K.; Lee, C.; Lee, G. H.; Hone, J.; Heinz, T. F.; Shan, J. *Nat. Mater.* **2013**, *12*, 207.
(18) Ross, J. S.; et al. *Nat. Commun.* **2013**, *4*, 1474.
(19) Fuchs, G.; Schiedel, C.; Hangleiter, A.; Härle, V.; Scholz, F. *Appl. Phys. Lett.* **1993**, *62*, 396.
(20) Sermage, B.; Chemla, D. S.; Sivco, D.; Cho, A. Y. *IEEE J. Quantum Electron.* **1986**, *22*, 774.
(21) Haug, A. *Semicond. Sci. Technol.* **1992**, *7*, 1337.
(22) Klimov, V. I.; Mikhailovsky, A. A.; McBranch, D. W.; Leatherdale, C. A.; Bawendi, M. G. *Science* **2000**, *287*, 1011.
(23) Wang, F.; Dukovic, G.; Knoesel, E.; Brus, L. E.; Heinz, T. F. *Phys. Rev. B* **2004**, *70*, 241403.
(24) Lueer, L.; Hoseinkhani, S.; Polli, D.; Crochet, J.; Hertel, T.; Lanzani, G. *Nat. Phys.* **2009**, *5*, 54.
(25) Valkunas, L.; Ma, Y. Z.; Fleming, G. R. *Phys. Rev. B* **2006**, *73*, 115432.
(26) Huang, L. B.; Krauss, T. D. *Phys. Rev. Lett.* **2006**, *96*, 057407.
(27) Exciton−exciton annihilation was reported very recently in the related TMD monolayer system of $MoSe_2$: Kumar, N.; Cui, Q.; Ceballos, F.; He, D.; Wang, Y.; Zhao, H. *Phys. Rev. B* **2014**, *89*, 125427.
(28) Lee, C.; Yan, H.; Brus, L. E.; Heinz, T. F.; Hone, J.; Ryu, S. *ACS Nano* **2010**, *4*, 2695.
(29) Mak, K. F.; Sfeir, M. Y.; Wu, Y.; Lui, C. H.; Misewich, J. A.; Heinz, T. F. *Phys. Rev. Lett.* **2008**, *101*, 196405.
(30) Shi, H.; Yan, R.; Bertolazzi, S.; Brivio, J.; Gao, B.; Kis, A.; Jena, D.; Xing, H. G.; Huang, L. *ACS Nano* **2013**, *7*, 1072.
(31) Kumar, N.; Cui, Q.; Ceballos, F.; He, D.; Wang, Y.; Zhao, H. *Nanoscale* **2014**, *6*, 4915.
(32) Cui, Q.; Ceballos, F.; Kumar, N.; Zhao, H. *ACS Nano* **2014**, *8*, 2970.
(33) Mai, C.; Barrette, A.; Yu, Y.; Semenov, Y. G.; Kim, K. W.; Cao, L.; Gundogdu, K. *Nano Lett.* **2013**, *14*, 202.

(34) Wang, Q.; Ge, S.; Li, X.; Qiu, J.; Ji, Y.; Feng, J.; Sun, D. *ACS Nano* **2013**, *7*, 11087.
(35) Sim, S.; Park, J.; Song, J. G.; In, C.; Lee, Y. S.; Kim, H.; Choi, H. *Phys. Rev. B* **2013**, *88*, 075434.
(36) Korn, T.; Heydrich, S.; Hirmer, M.; Schmutzler, J.; Schueller, C. *Appl. Phys. Lett.* **2011**, *99*, 102109.
(37) Lagarde, D.; Bouet, L.; Marie, X.; Zhu, C. R.; Liu, B. L.; Amand, T.; Tan, P. H.; Urbaszek, B. *Phys. Rev. Lett.* **2014**, *112*, 047401.
(38) Zhang, X.; You, Y.; Zhang, F.; Hone, J.; Heinz, T. F. *Bull. Am. Phys. Soc.* **2014**, *C1*, 168 (Abstract ID: BAPS.2014.MAR.C1.168).
(39) Brendel, M.; Kruse, A.; Jönen, H.; Hoffmann, L.; Bremers, H.; Rossow, U.; Hangleiter, A. *Appl. Phys. Lett.* **2011**, *99*, 031106.

dx.doi.org/10.1021/nl5021975 | *Nano Lett.* 2014, 14, 5625−5629